atoms

MDPI

Article

Resolution Characterizations of JetRIS in Mainz Using ^{164}Dy

Danny Münzberg [1,2,3,*], Michael Block [1,2,3], Arno Claessens [4], Rafael Ferrer [4], Mustapha Laatiaoui [3], Jeremy Lantis [3], Steven Nothhelfer [1,2,3], Sebastian Raeder [1,2] and Piet Van Duppen [4]

1 GSI Helmholtzzentrum für Schwerionenforschung GmbH, 64291 Darmstadt, Germany; m.block@gsi.de (M.B.); nothhelfer@uni-mainz.de (S.N.); s.raeder@gsi.de (S.R.)
2 Helmholtz-Institut Mainz, 55099 Mainz, Germany
3 Department Chemie, Johannes Gutenberg-Universität Mainz, 55099 Mainz, Germany; mlaatiao@uni-mainz.de (M.L.); jlantis@uni-mainz.de (J.L.)
4 KU Leuven, Instituut Voor Kern-en Stralingsfysica, B-3001 Leuven, Belgium; arno.claessens@kuleuven.be (A.C.); rafael.ferrer@kuleuven.be (R.F.); piet.vanduppen@kuleuven.be (P.V.D.)
* Correspondence: dmuenzbe@students.uni-mainz.de

Abstract: Laser spectroscopic studies of elements in the heavy actinide and transactinide region help understand the nuclear ground state properties of these heavy systems. Pioneering experiments at GSI, Darmstadt identified the first atomic transitions in the element nobelium. For the purpose of determining nuclear properties in nobelium isotopes with higher precision, a new apparatus for high-resolution laser spectroscopy in a gas-jet called JetRIS is under development. To determine the spectral resolution and the homogeneity of the gas-jet, the laser-induced fluorescence of ^{164}Dy atoms seeded in the jet was studied. Different hypersonic nozzles were investigated for their performance in spectral resolution and efficiency. Under optimal conditions, a spectral linewidth of about 200–250 MHz full width at half maximum and a Mach number of about 7 was achieved, which was evaluated in context of the density profile of the atoms in the gas-jet.

Keywords: JetRIS; fluorescence spectroscopy; gas-jet; de Laval nozzle; nobelium

Citation: Münzberg, D.; Block, M.; Claessens, A.; Ferrer, R.; Laatiaoui, M.; Lantis, J.; Nothhelfer, S.; Raeder, S.; Van Duppen, P. Resolution Characterizations of JetRIS in Mainz Using ^{164}Dy. *Atoms* **2022**, *10*, 57. https://doi.org/10.3390/atoms10020057

Academic Editor: Jean-Christophe Pain

Received: 29 April 2022
Accepted: 25 May 2022
Published: 28 May 2022

1. Introduction

The measurement of atomic transitions via laser spectroscopy is a versatile method for determining fundamental nuclear and atomic properties [1–4]. At the GSI Helmholtzzentrum für Schwerionenforschung, Darmstadt, Germany, laser spectroscopy is used at the Separator for Heavy Ion reaction Products (SHIP) [5,6] with a focus on the heavy actinide and transactinide region [4,7,8]. The low production rates and short half-lives of these nuclides pose difficult experimental challenges and require highly sensitive techniques. Recent laser spectroscopic measurements were conducted successfully at GSI on nobelium isotopes produced through fusion-evaporation reactions at SHIP using the Radiation Detected Resonance Ionization Spectroscopy (RADRIS) technique [7,9], where reaction products are thermalized in an argon filled gas cell and collected on a tantalum filament. The ions are neutralized by collection on a metallic filament, which is subsequently heated to produce an atomic vapor for resonance ionization spectroscopy (RIS). Due to the pressure and temperature conditions in the gas cell, the spectral resolution is limited to about 3 GHz. This is often insufficient to resolve all individual hyperfine components of the studied optical transition, as, e.g., in the case of ^{253}No [10]. Additionally, species with half-lives of less than approximately one second are inaccessible to the RADRIS technique due to decay losses during recoil ion collection. To overcome both of these limitations, JetRIS has been constructed for high-resolution resonance ionization spectroscopy in a hypersonic gas-jet [10]. JetRIS combines the high resolution of the in-gas-jet laser spectroscopy technique developed at KU Leuven [11–13] with the sensitivity of the ion collection and neutral desorption from a heated filament used in the RADRIS technique [14,15]. In the new approach presented here, after neutralization, the atoms are carried through a hypersonic nozzle to form a

low-temperature and low-density gas-jet, reducing the Doppler and collisional broadening effects and thus increasing the spectral resolution by an order of magnitude. The ability to transport neutral species makes it possible to run the system in a continuous mode instead of in cycles as is happening in RADRIS. The negative potential on the filament can be applied at all times in addition to heating, minimizing the before-mentioned decay losses. JetRIS is designed to achieve a spectral resolution of at least 400 MHz for the heaviest elements, allowing for a more precise determination of the nuclear moments. To understand the performance of different nozzles, we present here the characteristics of these in terms of Mach number, spectral resolution and homogeneity of the produced jet.

2. Experimental Procedure

2.1. A Technical Overview of JetRIS

JetRIS consists of a high-pressure gas cell (stagnation pressure P_0 of 80–125 mbar argon) used to stop and thermalize recoil ions from fusion-evaporation reactions after separation from the primary beam by SHIP and a lower pressure jet cell (background pressure P of 5×10^{-3} mbar–2×10^{-2} mbar), which is used for laser spectroscopy. Inside the gas cell, the thermalized ions are transported via an electric field created by a set of cylindrical electrodes toward a filament located at the front of the nozzle, as sketched in Figure 1. This filament, typically made of tantalum, is resistively heated, allowing for neutralization and desorption of atoms, which are subsequently transported by a gas flow into the jet cell through the de Laval nozzle, forming a well-collimated hypersonic gas-jet. This gas-jet features a low temperature and a low pressure, thus reducing the spectral linewidth while the collimation of the gas-jet is crucial to maintain the highest efficiency. Two laser beams are used in a cross-beam geometry to interact with the gas-jet, performing two-step resonance ionization spectroscopy. The laser for the first excitation step is propagating anticollinearly relative to the gas-jet, while the second step proceeds in a perpendicular configuration. While the perpendicular configuration reduces the power density of the laser light, it helps in avoiding ionization in the gas cell. The photo-ions are then guided around a 90° curve via a radio frequency quadrupole (RFQ) to a detector cell, where a channel electron multiplier (CEM) or silicon detector is located. A more detailed description of JetRIS can be found in [10]. In this technique, the nozzle determines the achievable resolution and the total efficiency from the collimation. Therefore, a thorough characterization is essential in understanding the performance of the setup. At KU Leuven, such nozzles are studied in detail using Laser Induced Fluorescence (LIF) in Cu I using pulsed laser radiation as well as the RIS of neutral Cu atoms [16,17].

In this study, we follow a different path by using LIF of neutral ^{164}Dy, which is illuminated by light from a cw-diode laser, propagating anticollinearly to the gas-jet as sketched in Figure 2. With this technique, three different de Laval type nozzles were investigated, and they were designed for different operation pressures and differences in their contour. All of them feature a throat diameter of 1 mm. The first nozzle is intended for usage at low stagnation pressures of P_0 = 80 mbar and a background pressure of $P = 2.5 \times 10^{-2}$ mbar. The diverging part of this nozzle has a length of about 1 cm as sketched in Figure 3. From fluid dynamic calculations, a jet of approximately Mach 8 was expected. The second nozzle is optimized for high stagnation pressures around P_0 = 300 mbar, and here, the diverging part has a length of about 3 cm. This nozzle is identical to the nozzles investigated recently at KU Leuven [16]. The third nozzle, referred to as the mid-range nozzle, has a conic contour. Here, the diverging part has a length of 2 cm. This nozzle was a prototype for operation in an intermediate pressure range while being simple to machine. No simulations were performed to optimize the design of this nozzle, and its optimal operating conditions were not previously known. To seed the atoms into the gas-jet for these tests, the tantalum filament in front of the nozzle was replaced by a tantalum strip that was previously loaded with a sample and resistively heated until a suitable fluorescence signal was observed, but the temperature of the filament was not

measured. It can only be approximated from its color when glowing, with an estimated temperature of 1200 °C.

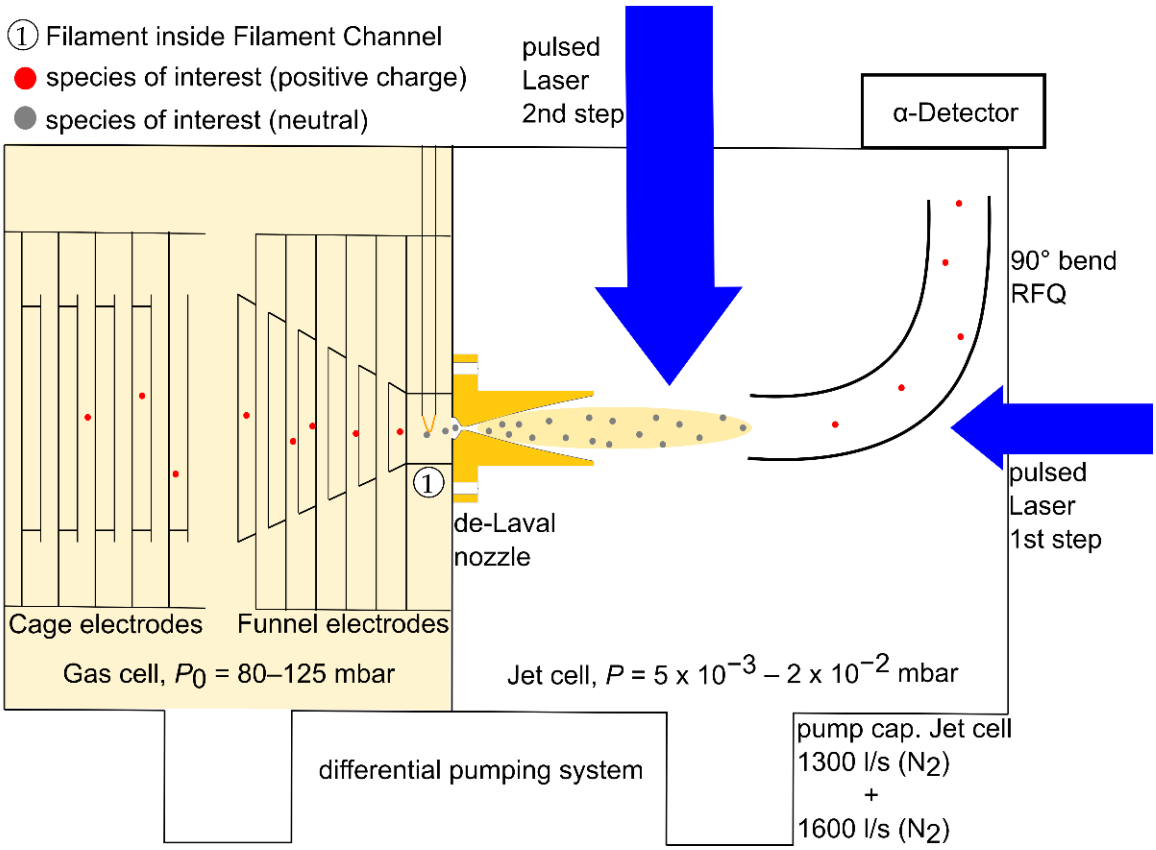

Figure 1. Schematic overview of JetRIS. On the left side are the cage and funnel electrodes. In front of the nozzle, there is a tantalum filament. After being evaporated from the filament, the atoms follow the flow of the buffer gas through the nozzle into the gas-jet. Here, two laser beams used in a cross-beam geometry resonantly ionizes the formerly neutralized species of interest. The ions are guided around a curve via a 90° bend RFQ and collected on an α-Detector.

2.2. Fluorescence Characterization

During the experiments presented in this work, we used one-step laser excitation in contrast to the two-step resonant ionization that will be used in online experiments. As no ions were produced, the RFQ structure was removed (*cf.* Figure 2) and the fluorescence of the seeded atoms provided a way to determine the density and homogeneity along the gas-jet. The atom source was installed next to the nozzle entrance in the gas cell, consisting of a folded piece of tantalum foil, which contained a piece of a few mg of ^{164}Dy with an isotopic purity of about 95%. The usage of an isotopically enriched sample ensured the investigation of a single atomic line as only minor contributions to the fluorescence signal from other isotopes are present and the even-even isotope features no hyperfine structure splitting. The foil was resistively heated with an electric power of 15 W to produce a dysprosium vapor, which was carried to the nozzle by the gas flow. A self-built laser with a 405 nm laser diode (Thorlabs L405P20) in an external cavity in Litrow configuration with approximately 12 mW of laser power and a sub-megahertz linewidth was used to excite the $4f^{10}6s^2 \rightarrow 4f^{10}6s6p$ transition in Dy I at a wavelength of 404.5 nm and with a transition strength of 1.92×10^8 s^{-1} [18]. The laser beam was expanded to form a circle of about 10 mm in diameter and was aligned to propagate anticollinear to the central axis of the gas-jet. A Complementary Metal-Oxide Semiconductor (CMOS) camera (Zelux® CS 165 MU) with a quantum efficiency of 50% was used to capture the fluorescence light originating from the atomic deexcitation. A bandpass filter featuring about 40% transmission at 405 nm

and a bandwith of 10 nm was installed in front of the camera. Pictures of the fluorescence, as shown in Figure 4, were taken as a function of gas pressure, wavelength and exposure time, which did not exceed 26 s due to limitations of the software for the camera.

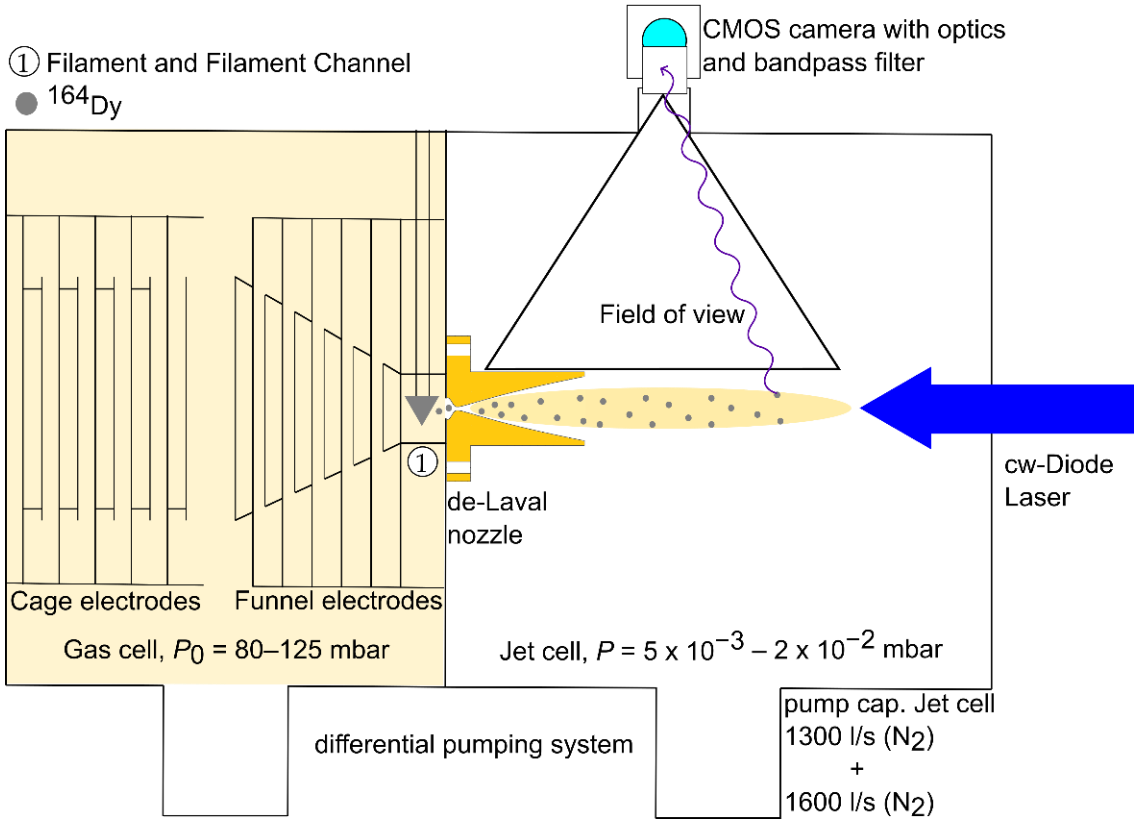

Figure 2. Schematic overview of JetRIS. On the left side are the cage and funnel electrodes, which are necessary for an online experiment but were not in use for the fluorescence measurements. In front of the nozzle, there is a tantalum filament that contains a piece of ^{164}Dy foil. After being evaporated from the filament, the atoms follow the flow of the buffer gas through the nozzle into the gas-jet. Here, a cw-diode laser beam at approximately 405 nm wavelength resonantly excites the dysprosium, and the resulting fluorescence is captured using a CMOS camera. The camera was mounted at a 45° angle relative to the field of view of this schematic.

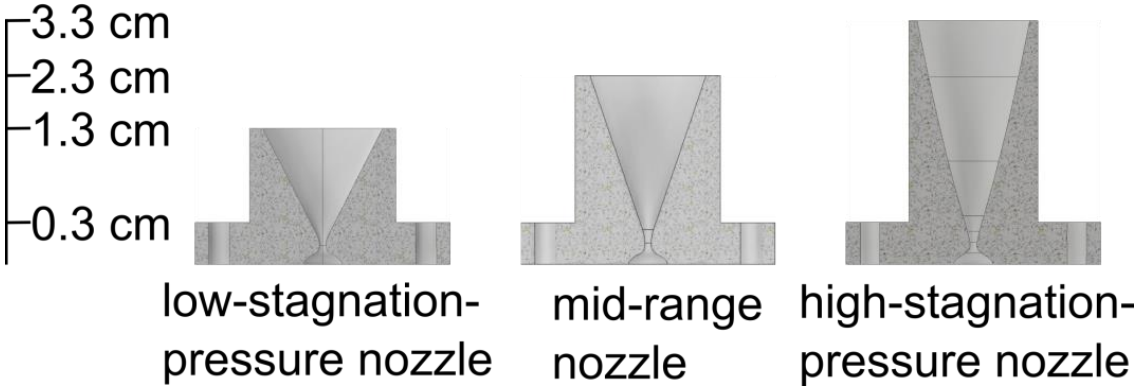

Figure 3. Cross sectional profiles of the characterized nozzles. The base and the diameter of the hole are identical for every nozzle.

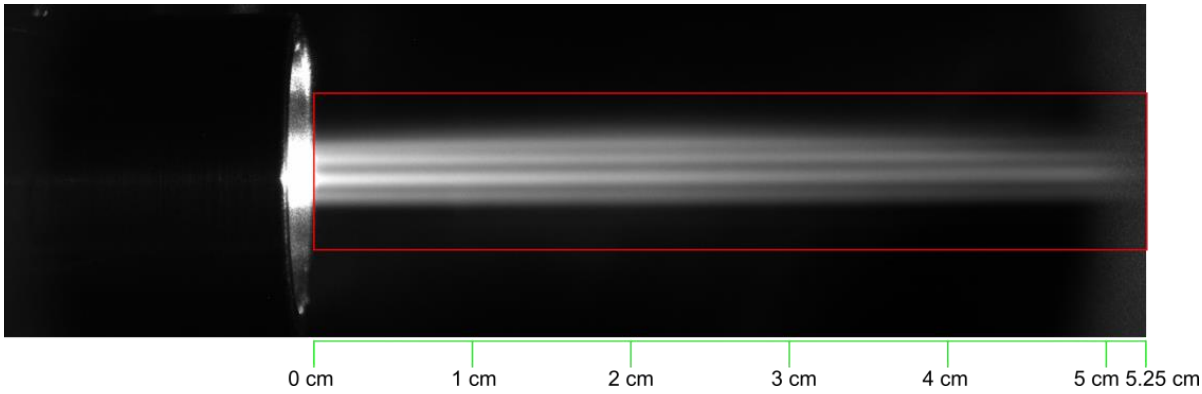

Figure 4. Example picture of the fluorescence acquired with the CMOS camera. Shown is the mid-range nozzle at the centroid frequency of the transition using a stagnation pressure of 100 mbar and a background pressure of 6.47×10^{-3} mbar. The visible stripes in the jet are a property of the laser diode used. The red box indicates the region that was considered in the analysis.

The fluorescence intensity was averaged in the radial plane, normal to the flow direction, in order to obtain information of the performance characteristics along the jet. Due to averaging, the stripes visible in Figure 4 did not disrupt the analysis.

2.3. Characterization of the Gas-Jet

The recorded fluorescence intensity was used to determine the density of atoms in the gas-jet, as well as to study the effective spectral broadening and, thus, the temperature of the jet, while exciting the atoms around the resonance frequency, i.e., performing spectroscopy. The intensity was evaluated pixelwise along the length of the gas-jet with the intensity averaged across the jet for each pixel in x direction. For each pixel, the normalized fluorescence intensity was plotted as a function of the laser frequency. A Gaussian fit to the data provided the centroid frequency and the spectral linewidth of the resonance. A number typically used to describe a gas-jet is the Mach number M, which is defined as the quotient of the stream velocity and the local speed of sound. It gives us an easy-to-compare variable that convolutes the speed of the jet and the temperature. The Mach number M is calculated with the following [11].

$$M = \sqrt{\frac{2}{\gamma - 1}\left(\frac{T_0}{T} - 1\right)}. \tag{1}$$

Here, γ is the ratio of the specific heat capacities of the gas, which is 5/3 for a monoatomic gas, T is the temperature of the jet and T_0 is the initial temperature of the gas before it reaches the nozzle.

The temperature T of the jet was determined from the measured linewidth by using the following relation.

$$\Delta\nu_{\mathrm{D}} = 2\sqrt{\ln(2)}\frac{\nu_{01}}{c}\sqrt{\frac{2kT}{m}}. \tag{2}$$

Here, $\Delta\nu_{\mathrm{D}}$ is the contribution to the full width at half maximum (FWHM) of the Doppler broadening, ν_{01} is the transition frequency, c is the speed of light, k is the Boltzmann constant and m is the mass of ^{164}Dy. As the measured resonance features a Voigt profile, the Doppler broadening can be determined by using the following approximate relation.

$$\Delta\nu = 0.5346\,\Delta\nu_{\mathrm{L}} + \sqrt{0.2166\,\Delta\nu_{\mathrm{L}}{}^2 + \Delta\nu_{\mathrm{D}}{}^2}. \tag{3}$$

Here, $\Delta\nu$ is the FWHM of the measured Voigt profile, and $\Delta\nu_{\mathrm{L}}$ describes the Lorentzian part of the overall resolution, which contains the natural linewidth and the pressure broadening. Any contribution from power broadening is neglected.

To obtain an estimate of the temperature T_0, the connection between T_0 and the stream velocity was used [11].

$$u = \sqrt{\frac{\gamma k T_0 M^2}{m(1 + \left(\frac{\gamma-1}{2}\right)M^2)}}. \quad (4)$$

where m is the mass of the buffer gas, and u is the stream velocity of the jet, which can be obtained from the recorded centroid using the optical Doppler shift from the literature value for the transition of ν_{01} = 24,708.97 cm^{-1} [19]. The stated reference did not mention the isotope of dysprosium for the recorded value. Therefore, the transition was measured with JetRIS by shining a laser beam perpendicular to the flow direction of the gas-jet, which yields a value free from Doppler shift. The measured value was in agreement with the literature value reported in [19].

Above Mach 5, the stream velocity reaches 95% of its maximum. Since the Mach number was expected to be around 5–8, the mean value of these (M = 6.5) was taken as an approximation for T_0. The deviation of the temperatures obtained with M = 5 and M = 8 from the value at M = 6.5 is around 3% and was considered when determining the uncertainty of the experimentally determined Mach number. A typical value of T_0 obtained from the fitting of the data is 380 K, indicating some heating of the gas from the hot filament, a fact that was already observed in previous investigations in Leuven [16].

To determine the quality of the gas-jet, a new metric was established and will be referred to as the homogeneity factor H. The photon density of the fluorescence light was used to evaluate the homogeneity of the sample atom density across the full length of the jet and was compared to a hypothetical, perfectly homogenous jet of constant light intensity. For this new factor, two different integrals have been calculated. A normalized integral of the hypothetical perfect jet $\int I_{\max}$, where the intensity should be constant over the entire length of the jet and the intensity integral over the experimental intensity values $\int I$, resulting in the following equation.

$$H = \frac{\int I}{\int I_{\max}}. \quad (5)$$

The boundaries of both integrals are the same and are determined by the length of the real jet. The homogeneity factor provides a simple value between 0 and 1, where 0 would mean no observed fluorescence, meaning no formation of a jet, and 1 would mean that we would observe a perfectly homogenous jet.

For an overall view on the performance of a nozzle, the spectral resolution and M were multiplied by the relative intensity, summed up and divided by the sum of the relative intensities, therefore making an intensity-weighted average. The uncertainty of these parameters was determined as the standard deviation of the individual numbers.

3. Results

3.1. Resolution

The low-stagnation-pressure nozzle is a de-Laval nozzle and was designed for a stagnation pressure of P_0 = 80 mbar and a background pressure of $P = 2.5 \times 10^{-2}$ mbar [20]. However, while investigating the resolution as a function of the background pressure, as shown in Figure 5a for the low stagnation pressure nozzle, a lower background pressure was found to provide the best resolution. This general trend that the resolution is improving as the background pressure drops was observed for all three nozzles. It has to be noted that the available pressure ranges are limited by the capacity of the JetRIS pumping system. At optimal parameters, the best achievable resolution was 212 ± 4 MHz for the low-stagnation-pressure nozzle, 239 ± 13 MHz for the mid-range nozzle and 311 ± 15 MHz for the high-stagnation-pressure nozzle. These values are all intensity-weighted averages of the individual values for each pixel slice along the gas-jet. It was verified whether analyzing the jet as a whole has an impact on the values relative to the pixel-by-pixel analysis, and

both methods are in agreement with one another. The optimal stagnation pressure of 300 mbar for the high-stagnation-pressure nozzle could not be reached, again limited by the pumping system [16]. Under the available conditions, the low-stagnation-pressure and mid-range nozzle outperformed the high-stagnation-pressure nozzle with regards to the obtained resolution. All of the obtained spectral linewidths are smaller than the stated goal of 400 MHz [10]. The individual parameters for the measurements are summarized in Table 1.

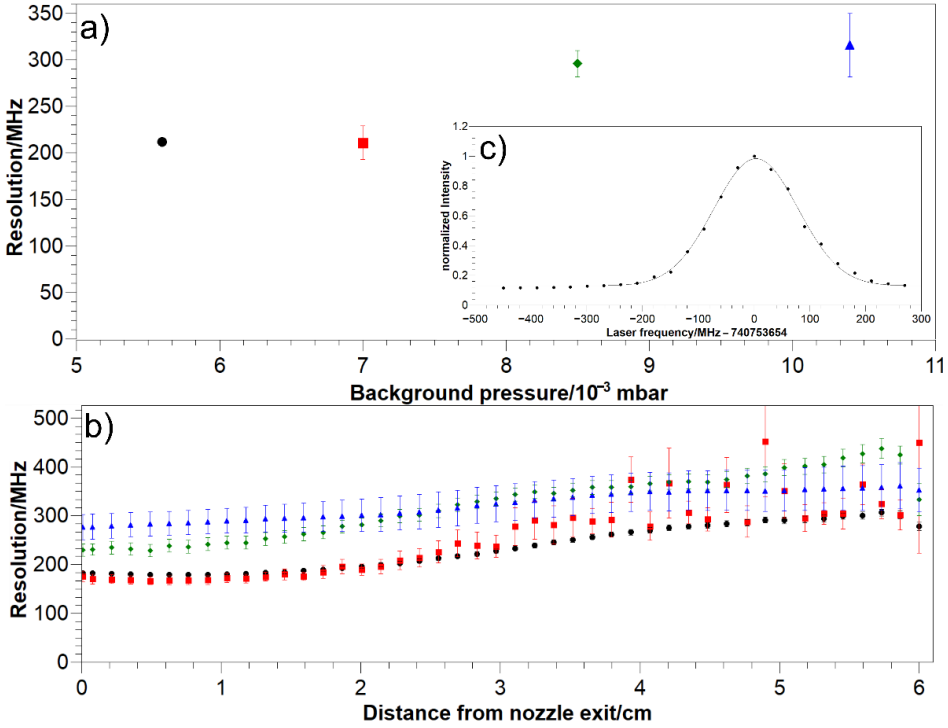

Figure 5. (**a**) Intensity-weighted averages of the resolution for the low-stagnation-pressure nozzle. The resolution generally improves as the background pressure is reduced. (**b**) Resolution along the jet for different parameters of the low-stagnation-pressure nozzle. (**c**) Example Gaussian fit of the intensity as a function of the laser frequency for the low-stagnation-pressure nozzle at P_0 = 80.6 mbar and $P = 5.6 \times 10^{-3}$ mbar. In both pictures, the parameters are as follows: black: P_0 = 80.6 mbar and $P = 5.6 \times 10^{-3}$ mbar; red: P_0 = 80.6 mbar and $P = 7.0 \times 10^{-3}$ mbar; green: P_0 = 80.0 mbar and $P = 8.5 \times 10^{-3}$ mbar; blue: P_0 = 82.2 mbar and $P = 10.4 \times 10^{-3}$ mbar.

Table 1. Intensity weighted averages of M, $\Delta\nu$ and H for the three different nozzles.

Nozzle	P_0/mbar	$P/10^{-3}$ mbar	M	$\Delta\nu$/MHz	H
Low-stagnation-pressure nozzle	80.6	5.6	7.2 ± 1.0	212 ± 30	0.40
	80.6	7.0	7.4 ± 1.0	211 ± 35	0.26
	80.0	8.5	5.0 ± 0.5	296 ± 33	0.43
	82.2	10.4	5.1 ± 0.7	316 ± 45	0.61
Mid-range nozzle	100	6.47	6.7 ± 0.9	250 ± 32	0.60
	125	7.35	7.2 ± 1.0	239 ± 33	0.67
	149	10.0	6.6 ± 0.9	259 ± 33	0.69
High-stagnation-pressure nozzle	125	9.3	4.2 ± 0.5	335 ± 31	0.84
	131	8.5	3.8 ± 0.3	352 ± 30	0.79
	154	12.2	4.6 ± 0.5	311 ± 34	0.78

3.2. Mach Number

The jet was evaluated for its Mach number as described in Section 2.3. For the determination of the gas-jet temperature from the linewidth, the spectral profiles were fitted with Gaussian profiles. The calculated linewidths were taken as the values for the overall resolution, since the fit was in good agreement with the data, as shown in Figure 5c. The natural linewidth can be calculated to be 30.5 MHz from the transition strength. The pressure broadening could not be determined; however, in the case of Cu I studied at Leuven, it was found to be approximately 3 MHz [16]. Power broadening has been neglected due to the low laser power used in the experiment. The two factors were added to a Lorentzian contribution to the linewidth of 33.5 MHz and the temperature-dependent part of the resolution was calculated according to Equation (3). With this, the Mach numbers were calculated as $M = 7.2 \pm 1.0$ for the low-stagnation-pressure nozzle, $M = 7.2 \pm 1.0$ for the mid-range nozzle and $M = 4.6 \pm 0.5$ for the high-stagnation-pressure nozzle in the best case, respectively. The Mach numbers of the high stagnation pressure nozzle are significantly lower than $M = 8$, expected from fluid-dynamics calculations and from observations at KU Leuven [16]. This was most likely due to the fact that the nozzle was used outside of its desired pressure range [21]. In this investigation, some small uncertainties in the evaluation remain, concerning the determination of the stagnation temperature T_0 and the frequency instability of the laser diode while measuring, which are expected to be reflected in the uncertainties. The presented values agree very well with the observations from previous studies at KU Leuven, albeit it has to be noted that the measurements were taken under different conditions. On one hand, the investigations in Leuven for the low-stagnation-pressure nozzle were performed using only the central 1 mm diameter of the gas-jet core with collinear illumination, while in this work the entire jet is illuminated anticollinearly, adding the jet boundary layer of the jet in the evaluation. Furthermore, the ^{164}Dy atoms used in this study are heavier than the ^{65}Cu atoms used in Leuven, which is a much lighter system that is closer to the carrier gas (^{40}Ar).

3.3. Homogeneity Factor

Finally, the homogeneity as defined in Equation (5) was evaluated, which shows a quite different behavior of the nozzles. With the best possible parameters, a value of $H = 0.33$ was achieved for the low-stagnation-pressure nozzle, compared to values of $H = 0.63$ for the mid-range nozzle and $H = 0.76$ for the high-stagnation-pressure nozzle. The corresponding intensity distributions along the jet for the three nozzles are shown in Figure 6.

Clearly, none of the investigated nozzles provide an ideal jet with a perfectly homogenous density profile and some losses from diffusion into the background gas are unavoidable. Furthermore, the intensity profile at the spectral maximum was compared with the intensity profile averaged over the spectral profile. The latter corresponds to the total density of the jet independent of the velocity distribution and shows a better homogeneity. Nevertheless, the profile at the maximum excitation frequency corresponds to the accessible fraction of the density and, thus, provides a better estimate on the expected efficiency. It shall be noted that the pulsed laser for the intended resonant ionization application features a significantly larger bandwidth of about 100 MHz compared to the sub-megahertz bandwidth of the cw diode laser used in this work [22]. This will enable addressing more atoms of the ensemble in the gas-jet and, thus, the effective homogeneity will be in between the two curves in the upper and lower panels of Figure 6, respectively.

The homogeneity factor provides a good impression about the achievable efficiency from the atom density along the gas-jet, but it does not yet provide conclusive information about the overall efficiency of JetRIS. Further measurements are planned, including the transport efficiency of atoms evaporated from the filament and transported through the nozzle to the detector at online-like conditions. For this, a radioactive recoil source will be used, since it releases ions at a known rate, allowing for a quantitative measurement, independent from ionization efficiency when using lasers.

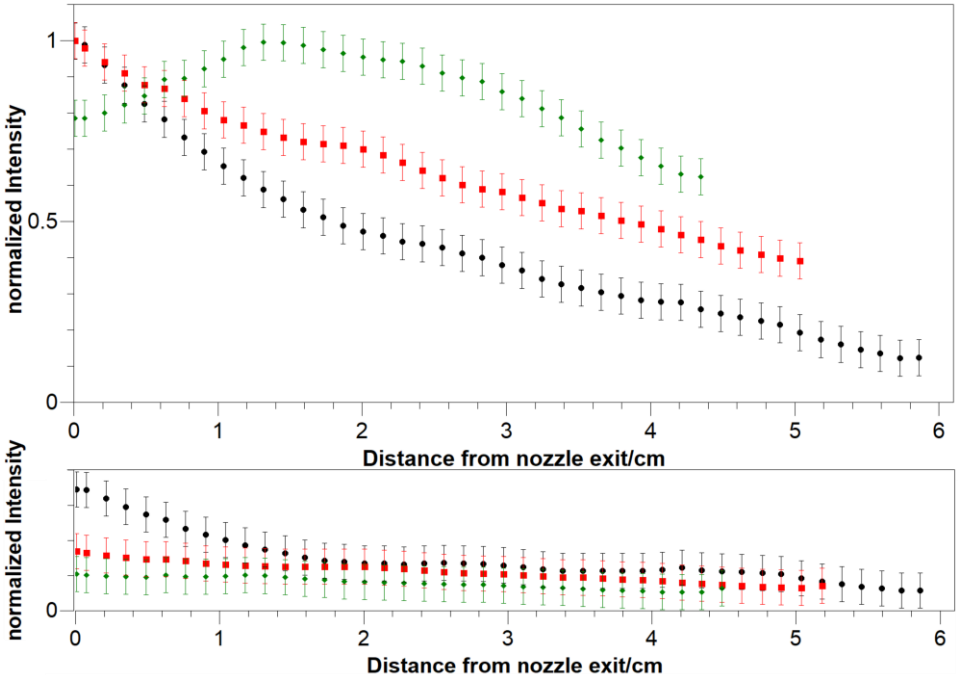

Figure 6. Intensity distribution at the centroid frequency (**upper**) and average over all frequencies (**lower**) for the best parameters of the low-stagnation-pressure nozzle (black, P_0 = 80.6 mbar, $P = 5.6 \times 10^{-3}$ mbar), mid-range nozzle (red, P_0 = 125 mbar, $P = 7.35 \times 10^{-3}$ mbar) and high-stagnation-pressure nozzle (green, P_0 = 125 mbar, $P = 9.3 \times 10^{-3}$ mbar).

4. Summary and Outlook

To enable high-resolution laser spectroscopy of the heaviest elements at GSI, Darmstadt JetRIS is under development. For an online experiment, efficiency is of paramount importance while maintaining a high spectral resolution. Therefore, fluorescence spectroscopy was performed to characterize three hypersonic nozzles in terms of spectral resolution, Mach number and homogeneity. These nozzles were designed for operation at different stagnation pressures. For each nozzle, gas pressures were identified resulting in a resolution sufficient for determining the hyperfine structure of ^{253}No, for example. The highest spectral resolution was found for the low-stagnation-pressure and the mid-range nozzle with linewidths of 211 MHz and 239 MHz, respectively, for the investigated ground-state transition at 404.5 nm in ^{164}Dy. In contrast, the high-stagnation pressure nozzle provided a linewidth of 335 MHz at the intended operation pressures of up to 125 mbar. The larger mass of ^{253}No compared to ^{164}Dy should allow achieving a higher resolution, but since the transition used for nobelium has a wavelength of 333 nm [7] compared to 405 nm for dysprosium, the resolution can be expected to be the similar in both cases. The low- and mid-range nozzle show a similar performance in terms of the Mach number as well. In terms of jet homogeneity, the high-stagnation-pressure nozzle showed the best performance. The mid-range nozzle seems to be the best overall choice, since its resolution and homogeneity are both close to the optimal values found for the other two nozzles. According to investigations at KU Leuven, the high-stagnation pressure nozzle would greatly benefit from operation at a higher stagnation pressure [16]. Nevertheless, our obtained resolution is already close to the value of 170 MHz projected in [16] for laser spectroscopy in the actinide region. Further studies will be performed offline with radioactive sources and resonance ionization spectroscopy to determine the efficiency of JetRIS before measuring online isotopes of nobelium at GSI, Darmstadt.

Author Contributions: R.F. and S.R. conceived the experiment. S.R., D.M., J.L. and S.N. set up the diode laser system. D.M., J.L. and S.N. conducted the measurements. D.M. and J.L. analyzed the data with the input from P.V.D., R.F., M.L., S.R., M.B. and A.C. The paper was written by D.M. with the input from P.V.D., M.B., A.C., R.F., J.L., M.L., S.N. and S.R. All authors have read and agreed to the published version of the manuscript.

Funding: M.L. acknowledges funding from the European Research Council (ERC) under the European Union's Horizon 2020 Research and Innovation Programme (Grant Agreement No. 819957).

Data Availability Statement: The data presented in this study are available upon request from the corresponding author.

Acknowledgments: The authors thankfully acknowledge the LARISSA group (Institut für Physik, Johannes Gutenberg-Universität Mainz) for the contribution of the laser diode cavity, as well as the target lab of GSI, Darmstadt, for the supply of enriched ^{164}Dy.

Conflicts of Interest: The authors declare no conflict of interest.

References

1. Kluge, H.-J.; Nörtershäuser, W. Lasers for nuclear physics. *Spectrochim. Acta B* **2003**, *58*, 1031–1045. [CrossRef]
2. Cheal, B.; Flanagan, K.T. Progress in laser spectroscopy at radioactive ion beam facilities. *J. Phys. G Nucl. Part. Phys.* **2010**, *37*, 113101. [CrossRef]
3. Campbell, P.; Moore, I.; Pearson, M. Laser spectroscopy for nuclear structure physics. *Prog. Part. Nucl. Phys.* **2016**, *86*, 127–180. [CrossRef]
4. Block, M.; Laatiaoui, M.; Raeder, S. Raeder. Recent progress in laser spectroscopy of the actinides. *Prog. Part. Nucl. Phys.* **2021**, *116*, 103834. [CrossRef]
5. Hofmann, S.; Münzenberg, G. The discovery of the heaviest elements. *Rev. Mod. Phys.* **2000**, *72*, 733–767. [CrossRef]
6. Münzenberg, G.; Faust, W.; Hofmann, S.; Armbruster, P.; Güttner, K.; Ewald, H. The velocity filter SHIP, a separator of unslowed heavy ion fusion products. *Nucl. Instrum. Methods* **1979**, *161*, 65–82. [CrossRef]
7. Laatiaoui, M.; Lauth, W.; Backe, W.L.H.; Block, M.; Ackermann, D.; Cheal, B.; Chhetri, P.; Düllmann, C.; Van Duppen, P.; Even, J.; et al. Atom-at-a-time laser resonance ionization spectroscopy of nobelium. *Nature* **2016**, *538*, 495–498. [CrossRef] [PubMed]
8. Backe, H.; Lauth, W.; Block, M.; Laatiaoui, M. Prospects for laser spectroscopy, ion chemistry and measurements of superheavy elements in buffer-gas traps. *Nucl. Phys. A* **2015**, *944*, 492–517. [CrossRef]
9. Lauth, W.; Backe, H.; Dahlinger, M.; Klaft, I.; Schwamb, P.; Schwickert, G.; Trautmann, N.; Othmer, U. Resonance Ionization spectroscopy in a buffer gas cell with radioactive decay detection, demonstrated using ^{208}Tl. *Phys. Rev. Lett.* **1992**, *68*, 1675–1678. [CrossRef] [PubMed]
10. Raeder, S.; Block, M.; Chhetri, P.; Ferrer, R.; Kraemer, S.; Kron, T.; Laatiaoui, M.; Nothhelfer, S.; Schneider, F.; Van Duppen, P.; et al. A gas-jet apparatus for high-resolution laser spectroscopy on the heaviest elements at SHIP. *Nucl. Instrum. Methods Phys. Res. Sect. B Beam Interact. Mater. At.* **2020**, *463*, 272–276. [CrossRef]
11. Kudryavtsev, Y.; Ferrer, R.; Huyse, M.; Bergh, P.V.D.; Van Duppen, P. The in-gas-jet laser ion source: Resonance ionization spectroscopy of radioactive atoms in supersonic gas jets. *Nucl. Instrum. Methods Phys. Res. Sect. B Beam Interact. Mater. B Beam Interact. Mater. At.* **2013**, *297*, 7–22. [CrossRef]
12. Raeder, S.; Bastin, B.; Block, M.; Creemers, P.; Delahaye, P.; Ferrer, R.; Fléchard, X.; Franchoo, S.; Ghys, L.; Gaffney, L.P.; et al. Developments towards in-gas-jet laser spectroscopy studies of actinium isotopes at LISOL. *Nucl. Instrum. Methods Phys. Res. Sect. B Beam Interact. Mater. At.* **2016**, *376*, 382–387. [CrossRef]
13. Ferrer, R.; Barzakh, A.; Bastin, B.; Beerwerth, R.; Block, M.; Creemers, P.; Grawe, H.; de Groote, R.; Delahaye, P.; Fléchard, X.; et al. Towards high- resolution laser ionization spectroscopy of the heaviest elements in supersonic gas jet expansion. *Nat. Commun.* **2017**, *8*, 14520. [CrossRef] [PubMed]
14. Laatiaoui, M.; Backe, H.; Block, M.; Chhetri, P.; Lautenschläger, F.; Lauth, W.; Walther, T. Perspectives for laser spectroscopy of the element nobelium. *Hyperfine Interact* **2013**, *227*, 69–75. [CrossRef]
15. Lautenschläger, F.; Chhetri, P.; Ackermann, D.; Backe, H.; Block, M.; Cheal, B.; Clark, A.; Droese, C.; Ferrer, R.; Giacoppo, F.; et al. Developments for resonance ionization laser spectroscopy of the heaviest elements at SHIP. *Nucl. Instrum. Methods Phys. Res. Sect. B Beam Interact. Mater. At.* **2016**, *383*, 115–122. [CrossRef]
16. Ferrer, R.; Verlinde, M.; Verstraelen, E.; Claessens, A.; Huyse, M.; Kraemer, S.; Kudryavtsev, Y.; Romans, J.; Bergh, P.V.D.; Van Duppen, P.; et al. Hypersonic nozzle for laser-spectroscopy studies at 17 K characterized by resonance-ionization-spectroscopy-based flow mapping. *Phys. Rev. Res.* **2021**, *3*, 043041. [CrossRef]
17. Zadvornaya, A.; Creemers, P.; Dockx, K.; Ferrer, R.; Gaffney, L.P.; Gins, W.; Granados, C.; Huyse, M.; Kudryavtsev, Y.; Laatiaoui, M.; et al. Characterization of Supersonic Gas Jets for High-Resolution Laser Ionization Spectroscopy of Heavy Elements. *Phys. Rev. X* **2018**, *8*, 041008. [CrossRef]

18. Wickliffe, M.; Lawler, J.; Nave, G. Atomic transition probabilities for Dy I and Dy II. *J. Quant. Spectrosc. Radiat. Transf.* **2000**, *66*, 363–404. [CrossRef]
19. Sansonetti, J.E.; Martin, W.C. Handbook of Basic Atomic Spectroscopic Data. *J. Phys. Chem. Ref. Data* **2005**, *34*, 1559–2259. [CrossRef]
20. Roelens, S. Characterization of a Hypersonic Nozzle for Laser Spectroscopy of Singly-Charged Thorium Ions. Master's Thesis, KU Leuven, Leuven, Belgium, 2021.
21. Verstraelen, E. Laser Spectroscopy of Actinides: Octupole Deformation and Gas-Jet Characterization. Ph.D. Thesis, Ku Leuven, Leuven, Belgium, 2021.
22. Verlinde, M.; Ferrer, R.; Claessens, A.; Granados, C.A.; Kraemer, S.; Kudryavtsev, Y.; Li, D.; Bergh, P.V.D.; Van Duppen, P.; Verstraelen, E. Single-longitudinal-mode pumped pulsed-dye amplifier for high-resolution laser spectroscopy. *Rev. Sci. Instrum.* **2020**, *91*, 103002. [CrossRef] [PubMed]